Theor Ecol
DOI 10.1007/s12080-014-0219-7

ORIGINAL PAPER

Evolution of acuteness in pathogen metapopulations: conflicts between "classical" and invasion-persistence trade-offs

Sourya Shrestha · Ottar N. Bjørnstad · Aaron A. King

Received: 20 February 2013 / Accepted: 4 February 2014

Abstract Classical life-history theory predicts that acute, immunizing pathogens should maximize between-host transmission. When such pathogens induce violent epidemic outbreaks, however, a pathogen's short-term advantage at invasion may come at the expense of its ability to persist in the population over the long term. Here, we seek to understand how the classical and invasion-persistence trade-offs interact to shape pathogen life-history evolution as a function of the size and structure of the host population. We develop an individual-based infection model at three distinct levels of organization: within an individual host, among hosts within a local population, and among local populations within a metapopulation. We find a continuum of evolutionarily stable pathogen strategies. At one end of the spectrum—in large well-mixed populations—pathogens evolve to greater acuteness to maximize between-host transmission: the classical trade-off theory applies in this regime. At the other end of the spectrum—when the host population is broken into many small patches—selection favors less acute pathogens, which persist longer within a patch and thereby achieve enhanced between-patch transmission: the invasion-persistence trade-off dominates in this regime. Between these extremes, we explore the effects of the size and structure of the host population in determining pathogen strategy. In general, pathogen strategies respond to evolutionary pressures arising at both scales.

Keywords Evolution of infectious pathogens · Invasion-persistence trade-off · Metapopulation model · Acute infections · Individual-based model · *Bordetellae*

S. Shrestha (✉) · A. A. King
Department of Ecology and Evolutionary Biology, University of Michigan, Ann Arbor, MI 48109, USA
e-mail: sourya@umich.edu

S. Shrestha · A. A. King
Center for the Study of Complex Systems, University of Michigan, Ann Arbor, MI 48109, USA

O. N. Bjørnstad
Department of Entomology and Biology, Pennsylvania State University, University Park, PA 16802, USA

A. A. King
Department of Mathematics, University of Michigan, Ann Arbor, MI 48109, USA

A. A. King · O. N. Bjørnstad
Fogarty International Center, National Institutes of Health, Bethesda, MD 20892, USA

Present Address:
S. Shrestha
Johns Hopkins School of Public Health, Baltimore, MD 21205, USA

Introduction

Infectious diseases afford perhaps the best illustrations of how natural selection can exert conflicting pressures at different scales of biological organization. The pathogen strategy that maximizes between-host transmission (as measured by the basic reproductive ratio, R_0) is classically considered to be the most fit. When a trade-off between rate and duration of transmission exists at the level of the individual infected host, this optimum is associated with intermediate pathogen loads and transmission rates (May and Anderson 1983; Ewald1993). In this case, overly "prudent" pathogens will tend to have low within-host abundance and

Published online: 29 April 2014

consequently transmit inefficiently, while overly aggressive pathogens, by multiplying rapidly within the host, will tend either to kill the host or to elicit early clearance by the host immune system, in either case abbreviating the infectious period.

This "classical" trade-off theory nicely illustrates how the presence of a transmission bottleneck introduces complexity into pathogen life-history evolution (Coombs et al. 2007, Gilchrist and Coombs 2006; Antia et al. 1994; Alizon and van Baalen 2005, Levin and Pimentel 1981). In comparison, free-living organisms represent a relatively simple case, in which, all else being equal, the strategy that maximizes the instantaneous rate of increase (r) is the most fit. In pathogens, however, the strategy that maximizes within-host population growth—and thus has the competitive advantage within the host—may yet be at a disadvantage overall relative to the strategy that maximizes host-to-host transmission. There is likewise the potential for conflicting selection pressures at higher scales of organization. The observation that acute immunizing infections such as measles were apparently unable to establish in humans until population aggregations of sufficient size and density arose (along with agriculture in the neolithic period; Black et al. 1974; Black 1975; Mira et al. 2006) has recently led to the notion of an "invasion-persistence" trade-off. Grenfell (2001) hypothesized that while acute immunizing infections have a competitive advantage early in an outbreak due to their ability to quickly invade a susceptible population, they may be disadvantaged late in the outbreak due to their greater tendency to go locally extinct during their deep post-epidemic troughs. Exploring this idea, King et al. (2009) developed a model explicitly linking within- and between-host dynamics to show that, depending on the shape of transmission's dose–response curve, the invasion-persistence trade-off has indeed the potential to influence life-history evolution through extinction-mediated group selection. Here we study this phenomenon in more detail, asking specifically which metapopulation conditions give rise to selection pressures discordant from those of the classical trade-off theory. Using a model that explicitly incorporates within-host dynamics, between-host transmission, and colonization and extinction at the metapopulation scale, we demonstrate that—depending on the configuration of the host metapopulation—pathogen life histories will evolve either to maximize between-host R_0 (if local populations are large) as predicted by the classical trade-off theory or adopt a more prudent strategy to increase the between-patch reproductive ratio, R_* (if local populations are small) according to the invasion-persistence trade-off. Thus, depending on circumstances, group selection in a metapopulation may override selection acting at the individual host scale to shape the life-history traits of acute immunizing infections in a manner analogous to that in which 'group' selection at the individual host scale can override within-host selection for greater virulence.

A number of theoretical studies have examined how the spatial structure of host populations affects pathogen evolution. When transmission is limited to local neighborhoods, Boots and Sasaki (1999) showed that "self-shading" behavior—wherein virulent pathogens quickly deplete their local neighborhoods of susceptible hosts—diminishes the chance of virulent strains spreading. Changes in the ratio of local to global contact rates, however, can allow virulence to spread or lead to evolutionary bistability of avirulent and virulent strains (Boots et al. 2004). In a similarly lattice-structured theoretical landscape, but allowing for waning of immunity, van Ballegooijen and Boerlijst (2004) studied on the evolution of self-organized spatial dynamics ranging from localized disease outbreaks to epidemics spreading in waves. Their model predicted evolution towards pathogen traits that maximize infection frequency (the number of times a host becomes infected), and not the maximization of R_0. Assuming a competition/persistence trade-off, Keeling (2000) showed analytically that competition between a locally fitter but more extinction-prone strain versus a less fit, less extinction-prone strain can lead either to domination by one strain or the other or to coexistence, depending on the strength of local and global transmission. King et al. (2009) showed that stylized yet biologically reasonable within-host mechanisms plausibly lead to selection for more acute pathogen life histories and, under some circumstances, to evolution that drives pathogens to the edge of their own extinction. At the edge of extinction, we speculated that further R_0-enhancing selection for acuteness could be countered by group selection because of frequent extinction of overly acute lineages. Beyond this speculation, however, King et al. (2009) did not explore how local extinction and selection for rapid invasion would combine to shape life-history strategies in a metapopulation context. In such a context, the number and sizes of local populations and rates of dispersal among them should together influence the dominance of invasion-persistence versus classical trade-offs in pathogen evolution. Herein we use a three-tiered model to explore how these aspects of spatial structure modulate the interaction between these potentially conflicting trade-offs.

A three-tiered model

Our hierarchical approach has three submodels (Fig. 1). First, we consider how a pathogen trait shapes the time-varying within-host infection intensity and infection duration. We then translate infection intensity to transmission via a dose–response curve relating shedding rate to transmission rate; this determines the pattern of outbreaks within each local host population. Finally, we integrate from local

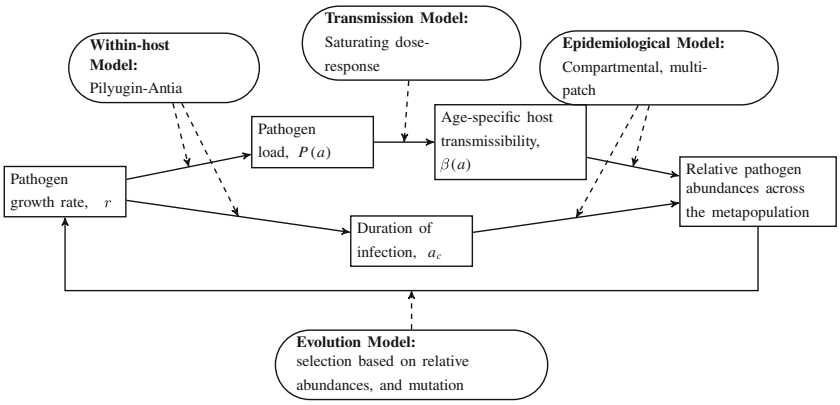

Fig. 1 Schematic representation of the three-tiered model. We consider the selective forces acting on a specific pathogen trait, namely the within-host proliferation rate, r. Under the dynamics prescribed by the within-host model (Eq. 1), this trait determines the duration of an infection, a_c, as well as pathogen load, P, over the infection's course. The transmission model translates within-host pathogen load to between-host transmission (Eq. 2). The epidemiological model then describes the progress of epidemics across the metapopulation. Mutation, together with differential survival and reproduction among pathogens ("Model for population structure and evolutionary dynamics" section), leads to natural selection on r

to regional dynamics using an epidemiological metapopulation model. The deterministic models for within-host dynamics are detailed in the "Models of within-host and transmission dynamics" section. In our earlier study (King et al. 2009), we used the McKendrick–von Foerster framework as a bridge between within-host dynamics to epidemiological dynamics. Here, in order to study evolution within the metapopulation, we implement instead a stochastic, individual-based model and simulate the progress of evolution explicitly. In this way, we allow both competition for susceptibles and extinction to shape pathogen evolution. The individual-based model is fully described in the "Model for population structure and evolutionary dynamics" section.

Models of within-host and transmission dynamics

We use a phenomenological description of the pathogen–immunity interactions to model within-host dynamics. The model is that studied by Pilyugin and Antia (2000), simplified to incorporate a linear functional response of the immune effectors (see also King et al. 2009). The pathogen load, P, and host immunity, X, are modeled as functions of the age of infection, a. Pathogen and host immunity interact in a predator–prey-like fashion according to the following:

$$\frac{dP}{da} = r\,P - k\,X\,P, \qquad \frac{dX}{da} = \alpha - d\,X + \gamma\,k\,X\,P, \quad (1)$$

where r is the pathogen intrinsic growth rate, k is the killing rate, γ measures proliferation of immune cells as a function of their encounter rate with pathogen, and α and d are background influx and death rates of immune cells, respectively. We assume that this system of differential equations is initiated with unit pathogen load in the absence of preexisting specific immunity, i.e., $P(0) = 1$, $X(0) = 0$. There are two dynamical regimes in this system with stable equilibria at (i) $P = 0$, $X = \alpha/d$ when $d/k < \alpha/r$, and (ii) $P = \frac{1}{\gamma}(d/k - \alpha/r)$, $X = r/k$ when $d/k > \alpha/r$ (Pilyugin and Antia 2000). En route to the second equilibrium, however, the parasite load, P, exhibits damped oscillations with transient excursions to biologically unrealistically low values. To remedy this, we assume a threshold parasite load, P_θ: when P first falls below the threshold, we interpret it as clearance. We set this clearance threshold to equal the inoculum size, i.e., $P_\theta = P(0) = 1$. It follows that there is a strain-specific but always finite period of infection, a_c, defined by the conditions $P(a_c) = 1$, $P(a) > 1$ for $0 < a < a_c$. Since the within-host dynamics are deterministic, each infection of a given pathogen strain follows the same dynamics. The strain-specific pathogen growth rate, r, plays a key role in shaping these dynamics: high values of r lead to acute but short-lived infections, while low r values result in mild, long-lasting infections (see Fig. 2 and King et al. 2009). The within-host pathogen model (Eq. 1) governs the infection intensity, P, within each infected host as a function of its infection age, a. We assume that the rate, β, at which an infected host transmits infection (the dose–response curve) is a saturating function of P according to

$$\beta(r, a) = q_s \left(1 - \exp\left(-\frac{P(r, a)}{P^*}\right)\right). \quad (2)$$

The parameters q_s and P^* are given in Table 1. Figure 2 shows how average transmission rate, infection duration, and R_0 depend upon r under this model. We discuss the alternative of a linear dose–response curve in the "Discussion" section.

Table 1 Synopsis of symbols

Symbol	Parameter	Value
Within-host model		
r	Parasite growth rate ("strategy")	3–60
r_0	The R_0 maximizing strategy	
r_*	The R_* maximizing strategy	
k	Kill rate of the immune response	3.5
α	Baseline production rate of immune response	1.0
d	Death rate of immune response	0.5
γ	Immune response recruitment rate	0.1
$\beta(a)$	Infection-age-specific transmission rate	
Transmission model		
q_s	Transmissibility factor	100.0
P^*	Saturation constant	−0.01
Population model		
N_P	Number of patches	1–300
n	Expected number of hosts in each patch	20–2,000
m	Migration rate	0.1
μ	Host birth rate	0.1
χ	Mutation rate (probability per transmission event)	0.01
σ	Mutation size (standard deviation)	0.35
R_0	The basic reproductive ratio	
R_*	The patch-level reproductive ratio	

Model for population structure and evolutionary dynamics

We use an individual-based approach that explicitly tracks each strain-specific infection. For simulations, we utilize a τ-leap algorithm (Higham 2008), with a small and fixed time-step, Δt, in lieu of more expensive event-driven simulations.

We subdivide the host population into N_P patches. The population size, n_j, of patch j varies stochastically according to a logistic birth–death process. The per capita host birth rate is constant and equal to μ, while the per capita host mortality rate is density dependent, equal to $\mu n_j/n$. Here, the parameter n is the expected patch size. Thus, in the interval Δt, each host in patch j faces a probability of death, $1-e^{-\mu(n_j/n)\Delta t}$. The number of births in the same interval is negative-binomially distributed with size parameter n_j and probability $e^{-\mu\Delta t}$. Newborns are all susceptible.

We assume that host migration is independent of infection status and that the population is globally connected so that migration is equally likely between all patches (at a

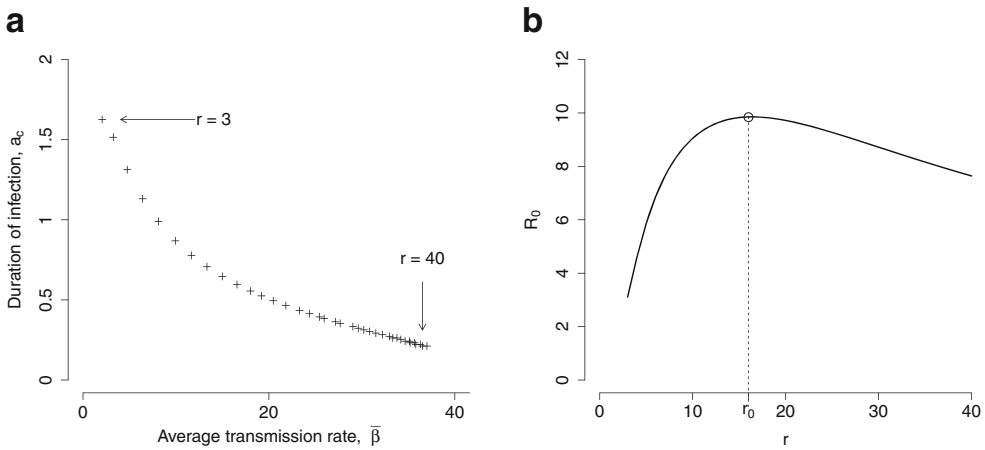

Fig. 2 Transmission rate, duration of infection, and R_0 in the combined within-host and transmission models. **a** The within-host proliferation parameter, r, controls both average transmission rate and infection infectious period. Infections become more acute as r increases. At the same time, peak pathogen load increases. **b** Within-host dynamics filtered by the transmission dose–response curve leads to maximization of the basic reproduction ratio, R_0, for intermediate values of r

constant rate m). Thus, the number of hosts that emigrate from patch j in a small time interval Δt is binomially distributed with parameters n_j, $p = 1 - e^{-m\,\Delta t}$.

Transmission is assumed to occur exclusively within patches. Pathogen strains are characterized by their within-host growth rate r, and infected hosts are differentiated by the pathogen strains they carry. We disallow coinfections. These assumptions ensure that the pathogen can evolve only in response to selection pressures at the between-host/within-patch and between-patch scales; unlike several recent studies (Coombs et al. 2007; Gilchrist and Coombs 2006), there is no within-host competition in our model. We further assume perfect cross-immunity between strains and lifelong immunity. Transmission is assumed to scale in a frequency-dependent fashion (e.g., Bjørnstad et al. 2002; Ferrari et al. 2011). This makes transmission rate, β, comparable across differing metapopulation configurations. Within a patch, a host infected with strain r exactly a time units ago carries a pathogen load $P(r, a)$ (Eq. 1) and contributes $\beta(r, a)$ to the total force of infection within that patch (Eq. 2). Although the number of allowable strains is unbounded, the number of strains circulating at any time is finite. The strain-specific force of infection for strain r in patch j in a metapopulation with N_P patches is

$$\lambda_{r,j} = \frac{1}{n_j} \sum_{\substack{\text{hosts } h \text{ in patch } j \\ \text{infected with strain } r}} \beta(r, a_h), \tag{3}$$

where a_h is the age of infection in host h. Thus, if s_j is the number of susceptible individuals in patch j and the total force of infection in patch j is $\lambda_j = \sum_r \lambda_{r,j}$, then the vector of new strain-specific infections, $\Delta i_j = (\Delta i_{r,j})$, occurring in patch j over the small time interval Δt, is distributed according to

$$\Delta i_j \sim \text{multinomial}(s_j, p_j), \tag{4}$$

where p_j is a vector of probabilities, $p_j = (p_{r,j})$ and $p_{r,j} = (1 - e^{-\lambda_j\,\Delta t})\,\lambda_{r,j}/\lambda_j$ is the probability that a patch-j susceptible becomes infected with strain r. Thus, competition among strains for susceptibles within each patch is governed by both strain frequency and strain-specific transmission rate, since $\lambda_{r,j}$ depends on both of these quantities.

In the model, the diversity of strains is reduced by competition and increased by mutation. During each transmission event, we assume that an offspring from a strain with $r = r_1$ will mutate to $r = r_2$ with probability χ. The value r_2 of the mutant is drawn from a normal distribution with mean r_1 and standard deviation σ.

One thousand replicate simulations were performed for each set of parameters. Each simulation run was initialized by infecting 1 % of the hosts randomly across the metapopulation, each with a single strain with a growth rate drawn from a uniform distribution on the interval (3, 10). Simulations were conducted in two phases. In the first phase, the simulation proceeded until transients died out. In the second phase, 1,000 replicate simulations were performed with mutation, each beginning from the distribution of the extant strains at the end of the first phase. These simulations are run for 2,000 time units, a sufficient amount of time to ensure that the strain distribution has stabilized. In all simulations, we use a time-step $\Delta t = 0.01$ time units.

Fitness measure, R_0

If we consider only a single patch ($N_P = 1$) and disallow mutation ($\chi = 0$), the model reduces to a stochastic version of the model described in the "McKendrick-von Foerster equations" section in the Appendix. In this setting, a pathogen with growth rate r, has a basic reproductive ratio,

$$R_0 = \int_0^{a_c} \beta(r, a)\, \exp(-\mu\, a)\, \mathrm{d}a, \tag{5}$$

where $\beta(r, a)$ is as defined in Eq. 2. Numerical integration of Eqs. 1, 2, and 5 yields the dependence of the R_0 on r. Figure 2b shows this dependence. R_0 reaches a maximum at an intermediate $r = r_0$; diminishing returns due to the saturating dose–response curve reduce R_0 beyond this point (see King et al. 2009 for a detailed discussion).

Model for patch dynamics

To obtain some insight retrospectively into the scenario with many small patches, we can reason by analogy that the host patches are, themselves, similar to infected hosts and the migration of infected hosts comparable to the host–host transmission process. This leads to the following set of equations, which can be viewed as an approximation to the patch-to-patch transmission dynamics:

$$\begin{aligned}
\frac{dS_P}{dt} &= f(\mu)\, R_P - \bar{\iota}\, m\, n\, S_P \frac{I_P}{N_P} \\
\frac{dI_P}{dt} &= \bar{\iota}\, m\, n\, S_P \frac{I_P}{N_P} - \frac{1}{\bar{\delta}}\, I_P \\
\frac{dR_P}{dt} &= \frac{1}{\bar{\delta}}\, I_P - f(\mu)\, R_P
\end{aligned} \tag{6}$$

where, S_P, I_P, R_P, and N_P are the number of susceptible, infected, recovered, and total patches respectively; μ is the host birth rate; n is the local population size; m is the between-patch migration rate; $\bar{\iota}$ is the average proportion of infected hosts in an infected patch; and $\bar{\delta}$ is the average duration of an epidemic. Susceptible patches become infected when infected hosts move from an infected patch to a susceptible patch. The rate at which this happens depends on the between-patch migration rate, m, the average number of infected hosts in an infected patch, given by the product of

$\bar{\iota}$ and n, and the probability such patches exchange hosts, given by the product of S_P and I_P/N_P. An epidemic in a patch will last an average of $\bar{\delta}$ time units, at which point the patch becomes "recovered," i.e., temporarily refractory to outbreaks. The rate $f(\mu)$ that recovered patches turn susceptible is a function of the host turnover rate, μ. Following Ball et al. (1997) and Ball and Neal (2002), we define the patch-level reproductive ratio, R_*, as the average number of new infected patches resulting from a single infected patch. For our patch-level model,

$$R_* = \bar{\iota}\,\bar{\delta}\,m\,n. \tag{7}$$

Analytic expressions exist neither for $\bar{\iota}$ nor $\bar{\delta}$, but consistent deterministic and stochastic approximations can be computed for each, as shown in the "Approximation of epidemic sizes" section in the Appendix. Figure 3 shows R_* as a function of r; importantly, the strategy that maximizes R_0 ($r = r_0$) is distinct from that which maximizes R_* ($r = r_*$).

Results

In a single patch, pathogens evolve to maximize R_0

When $N_P = 1$, hosts mix homogeneously within the population. Diversity of pathogen strains is maintained through mutation events, and the strains that circulate compete against one another for susceptible hosts. In this case, we observe directional selection and slow convergence of the strain distribution to the evolutionarily stable strategy, $r = r_0$, the strategy maximizing R_0. Heightened in-host replication rates lead to shortened infectious periods, but less-than-proportionally higher transmission rates due to the saturating dose–response curve. Note that the trade-off here is not, as in the classical theory (e.g., Levin and Pimentel 1981), due to disease-induced mortality, but rather because more rapid in-host growth leads to faster immune clearance. Figure 4a shows the transient and steady-state behavior of the model as the strain distribution settles around $r = 16$. Figure 4b shows that this strategy coincides with the maximum R_0.

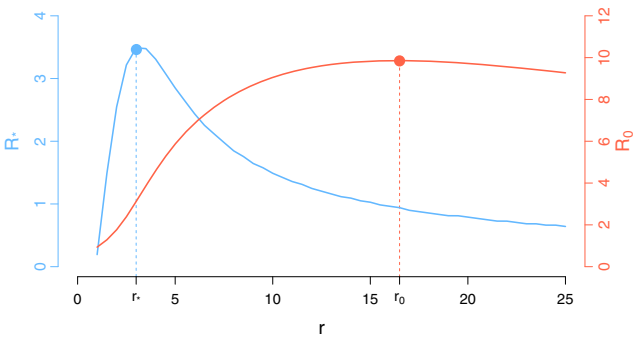

Fig. 3 R_0 and R_* have different optima. R_0 (*red curve*) is maximized at $r = r_0$, while R_* (*blue curve*) is maximized for $r = r_*$. Here, R_* is calculated with patch size, $n = 30$, and migration rate, $m = 0.1$. The left-hand axis relates to the *blue line*; the right-hand, to the *red*

In a metapopulation, conflicting selection pressures arise

When the host population is subdivided into smaller patches (N_P patches, each of mean size n), the R_0-maximizing $r = r_0$ is no longer optimal. As the patch size decreases, acute lineages become increasingly prone to local extinction, and as a result, the R_0-maximizing strains are selected against at the metapopulation level. Instead, more persistent strategies that increase between-patch spread are favored. Figure 5 shows how the evolutionarily stable strategy (ESS) varies over a range of metapopulation configurations. When the regional population size is too small, the pathogen goes extinct globally (crosses). Above this global extinction threshold, the ESS depends on the both N_P, and n and takes values between $r = r_0$ and $r = r_*$. Generally, when patches are large enough to support R_0-maximizing strains, the ESS approaches $r = r_0$ and when patches are small but numerous, the ESS approaches $r = r_*$. Transect B in Fig. 5 illustrates the effect of varying the metapopulation configuration while keeping the expected global host population size, $n\,N_P$, fixed. Transect C holds expected patch size fixed while varying the number of patches: the optimal strategy does not change, though the probability of global extinction declines as N_P increases. Transect D shows the effect of varying n while holding N_P fixed: optimal acuteness increases with the size of local patches. To summarize, both the number and size of patches determine the balance of the selection pressures arising at the two scales.

A sensitivity analysis of our results with respect to host demography (μ) and mobility (m) reveals, unsurprisingly, that increasing either parameter drives the ESS towards the within-patch optimum $r = r_0$. Increasing μ decreases local extinction rates, while making m larger tightens patch-to-patch coupling, effectively making the metapopulation more homogeneous (Fig. 8). We explored the effects of removing density-dependent host population regulation, thus allowing host populations to walk randomly. Under the resulting larger variation in local population sizes, more acute strains are favored in some regions of parameter space (cf. Fig. 10).

Discussion

In this study, we have taken a "bottom-up" approach to understanding the evolution of acuteness in pathogens as a function of the size and structure of the populations of their hosts. Our model connects three distinct levels of organization: within an individual host, between hosts within a

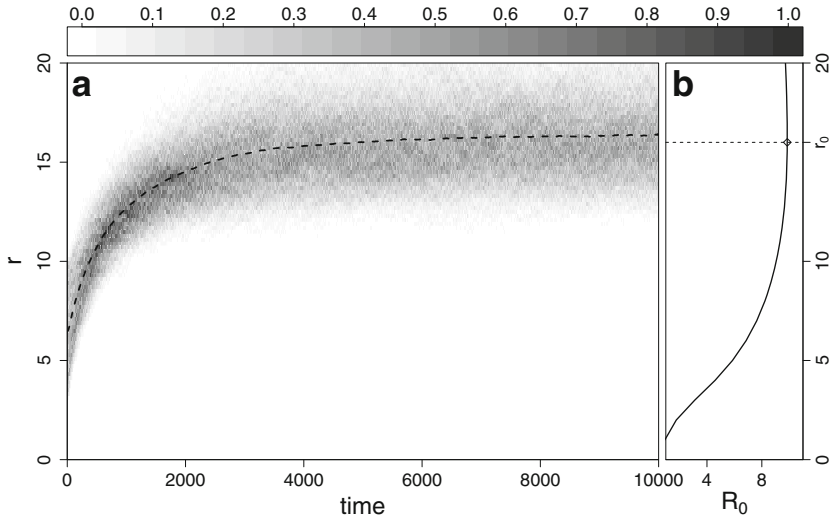

Fig. 4 An evolutionary trajectory. Simulation results for a single-patch model with 2,000 hosts. The *grayscale* indicates the distribution of $r(t)$ within the pathogen population; the *dashed line* plots the mean value of $r(t)$. Pathogens evolve to a evolutionarily stable $r = r_0$; this is equal to the r that maximizes the net reproductive number R_0. Sample trajectories for multi-patch configurations are shown in the Appendix

local population, and between local populations. We find that the structure of the host population is a critical determinant of the pathogen's evolution. Specifically, in larger and more well-mixed host populations, a pathogen's ESS shifts toward the strategy that maximizes between-host R_0; the classical trade-off theory applies in this regime. By contrast, in smaller, more patchy host populations, emergent metapopulation dynamics favor more persistent strategies; the invasion-persistence trade-off dominates in this regime. Between these extremes, the ESS reflects the balance of the conflicting pressures arising at the two scales.

Several authors have pointed out the shortcomings of R_0 as a measure of pathogen fitness in structured host populations. Ball et al. (1997) and Ball and Neal (2002) derived a threshold quantity for pathogen invasion in the context of several metapopulation models. We have retained their notation, R_*, for the patch-level reproductive ratio. Cross et al. (2005, 2007) found that, when host populations are patchy, R_* gives a more accurate prediction of the invasion threshold than R_0 does. Here, we have gone further to show that the ESS lies in general between the within-patch and between-patch optima and that patch size and number determine where on this continuum the evolutionarily stable acuteness falls.

The within-host model at the bottom of our three-level model hierarchy is only a caricature of infection dynamics, useful here inasmuch as it links a pathogen trait to the components of the pathogen's fitness and makes plain the trade-off between transmission rate and persistence. We chose this model because it and closely related models have been well studied (e.g., Gilchrist and Sasaki 2002; Ganusov and Antia 2003; Alizon and van Baalen 2005) and because it allows for direct connection with our earlier work (King et al. 2009). While our results are derived using a particular model, we expect that qualitatively similar conclusions would arise from other within-host models as long as (i) between-host transmission rate increases with pathogen load and (ii) more aggressive pathogens elicit faster clearance. In particular, under such conditions, selection at the within-patch level will, to a point, favor acute strains, while at the metapopulation level, the dynamics of local extinction and recolonization will exert a balancing pressure.

As in our earlier work (King et al. 2009), the shape of the dose–response curve (relating within-host intensity of infection to between-host transmission) is an important determinant of the pathogen's evolutionary trajectory. In this paper, we have focused on evolution under the assumption of a saturating curve because this affords the clearest illustration of the evolutionary tension between two well-defined strategies: that maximizing within-patch transmission vs. that maximizing between-patch spread. When the dose–response curve is nonsaturating, in contrast, R_0 increases monotonically with r, i.e., r_0 is effectively infinite. Selection at the within-patch level is thus for ever-increasing acuteness, continually pushing the pathogen toward more extinction-prone strategies. As illustrated in Fig. 6, under the assumption of a linear dose–response, regional persistence is much more frail and global extinctions more frequent. The saturating dose–response diminishes the advantage of extreme acuteness and thus yields greater regional persistence (cf. Fig. 6c–d vs. Fig. 5a). Rand et al. (1995) discussed a similar phenomenon.

Previous studies of pathogen evolution have shown that spatial structure may lead to evolutionary branching or bistability in pathogen traits (e.g., Boots et al. 2004). While this was not the focus of our study, we saw no such effects in the extensive numerical explorations we performed. This

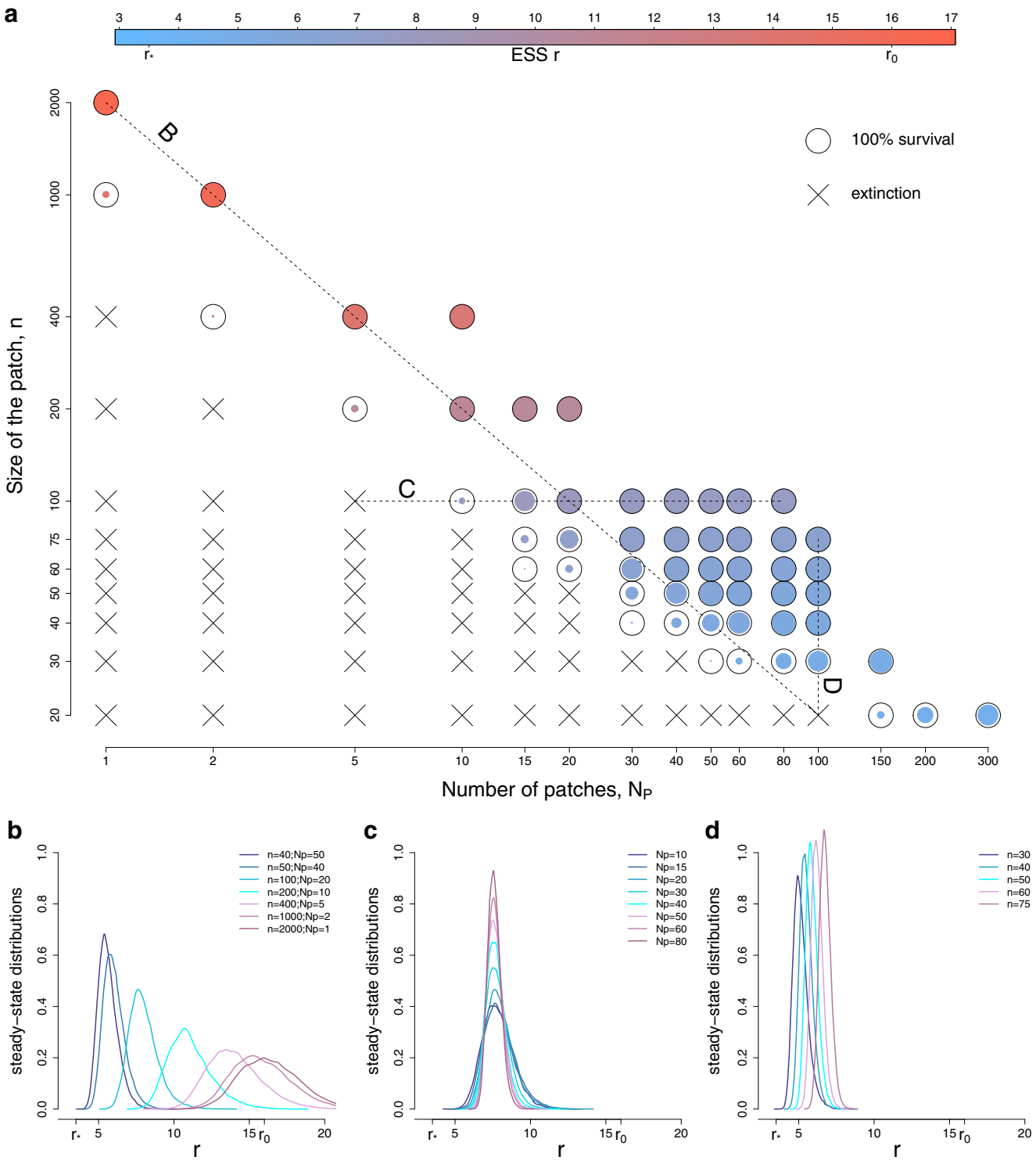

Fig. 5 Evolutionarily stable strategy (*ESS*) as a function of host population structure. **a** ESS *r* (mean *r* in the stable strain distribution, indicated by *color*) and survival fraction (chance of avoiding extinction by time 10,000, indicated by *symbol size*), at various metapopulation configurations. Metapopulations are characterized by size of patch, *n* (*vertical axis*) and number of patches, N_P (*horizontal axis*). *Black crosses* indicate extinction in all of 1,000 replicate runs by time 10,000. The *bottom panels* show steady-state strain distributions along three different transects across metapopulation structure. **b** The size and the number of patches vary, and the expected total regional population size remains constant at 2,000. **c** The number of patches varies, and the expected size of each patch remains constant at 100. **d** The size of patches varies, and the number of patches remains constant. Metapopulations with many large patches were not explored due to computational infeasibility

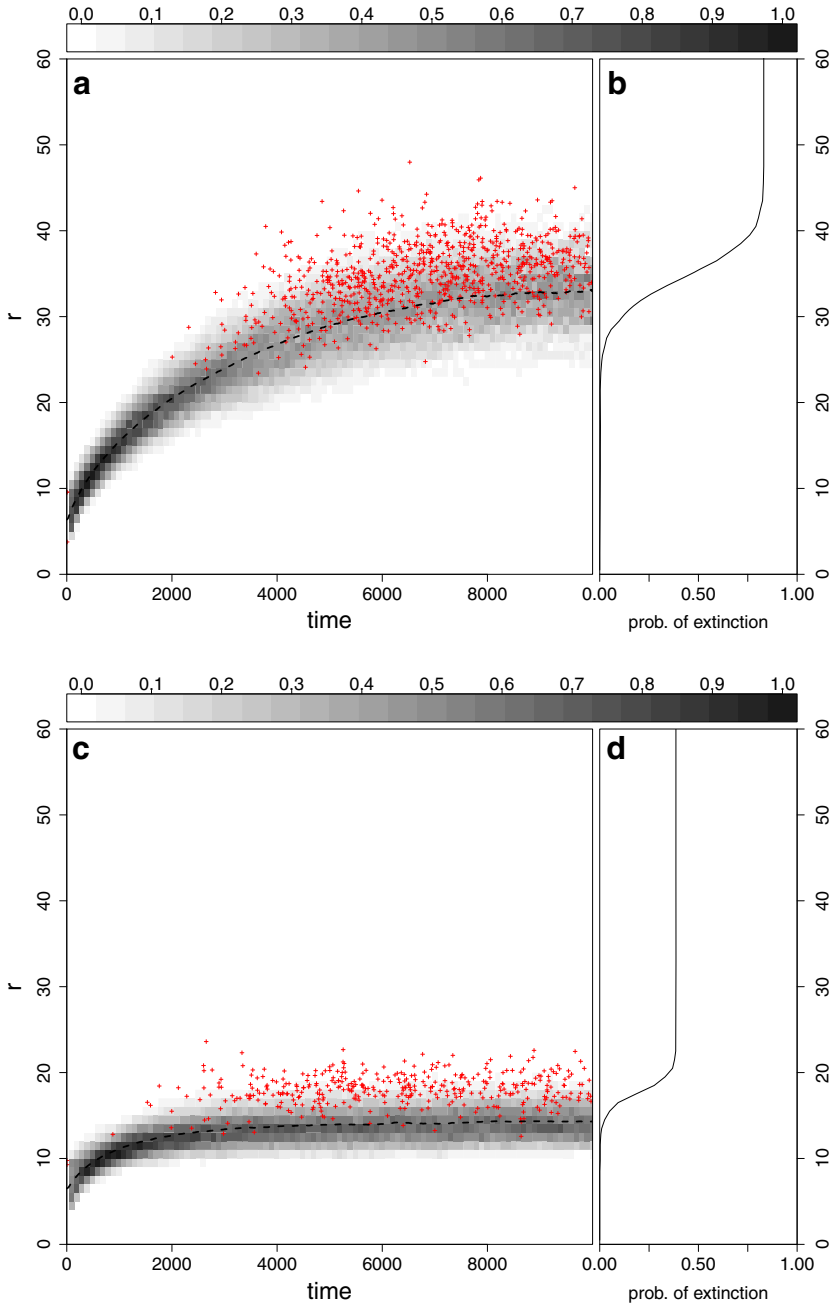

Fig. 6 Evolution to the edge of extinction. *Top panels* Simulation results for a single-patch model (initialized with 2,000 hosts) with a linear transmission dose–response curve, showing pathogen evolution through time. We construct the pathogen distribution at a given time, $r(t)$, by observing the average r of the pathogen present at that time, t, in each of the 1,000 simulations. In **a**, *shades of gray* shows the pathogen densities, and the *dashed line plots*, the average of the distribution $r(t)$. The evolutionary trajectory shows pathogen evolution towards higher acuteness. More acute strains become more prone to extinction; extinction events are indicated with *red crosses*. Probability of extinction (proportion of simulations that result in extinction) increases as r grows, as shown in **b**. **c**, **d** Simulation results for a multi-patch model (with 20 patches each with 100 hosts). The evolutionary trajectory to the edge of extinction, though for this configuration, the edge is associated with lower acuteness

may be because we assumed global mixing, thus preventing localized self-shading behavior (Boots and Sasaki 1999; Boots et al. 2004), disallowed superinfection (e.g., Boldin and Diekmann 2008), or excluded pathogen-driven mortality (e.g., Morozov and Best 2012). Interestingly, when we removed density-dependent host population regulation, thus allowing greater variation in size of patches, a greater diversity of strains were found to co-circulate in the metapopulation (Fig. 10). The role of extinction and hierarchical population structure in generating and maintaining polymorphism is an interesting area for future research (Svennungsen and Kisdi 2009).

Our study was originally motivated by the diverse life histories exhibited by bacteria of the genus *Bordetellae*. Two acute strains, *Bordetella pertussis* and *Bordetella parapertussis*, have emerged in humans from the less acute and persistent *Bordetella bronchiseptica* that infects a wide range of wild animals (Bjørnstad and Harvill 2005). In our previous work (King et al. 2009), we speculated that this was an illustration of the operation of the invasion-persistence trade-off via an implicit appeal to metapopulation dynamics. Here, through a more careful consideration of the evolutionary metapopulation context, we have explored how extinction and recolonization dynamics lead to conflicting selection

pressures at the local and metapopulation scales. In particular, we have shown how changing metapopulation structure can shift the balance between the classical and invasion-persistence trade-offs and that this shifting balance remains a viable hypothesis for the emergence and maintenance of acute pathogens.

Acknowledgments Financial support was provided by the Research and Policy for Infectious Disease Dynamics program of the Science and Technology Directorate, US Department of Homeland Security, and the Fogarty International Center, US National Institutes of Health. AAK acknowledges the support of the National Institutes of Health (grant #1-R01-AI-101155).

Appendix

McKendrick–von Foerster equations

We consider the spread of a disease in a well-mixed homogeneous population, where a transmission rate of a single host during an infection is varying, specified by the mechanistic model described earlier by Eq. 1. The transmission rate of a host infected a units of time ago is $\beta(a)$. Let $\int_{a_1}^{a_2} i(t,a)\,\mathrm{d}a$ be the fraction of host at time t infected between times $t-a_1$ and $t-a_2$. Then, the fraction of infected host at time t that have progressed a units into their infection follows:

$$\frac{\partial i}{\partial t} + \frac{\partial i}{\partial a} = -\mu(a)\, i, \qquad i(t,0) = \lambda(t)\, S(t), \tag{8}$$

where $\mu(a)$ is age-specific mortality, $\lambda(t)$ is the force of infection, and $S(t)$ is the fraction of the host population susceptible to infection at time t. The force of infection is

$$\lambda(t) = \int_0^{a_c} \beta(a)\, i(t,a)\,\mathrm{d}a = \int_0^{a_c} \beta(a)\, \ell(a)\, i(t-a,0)\,\mathrm{d}a. \tag{9}$$

Here, a_c is the time when the infection is cleared in the host, and $\ell(a) = \exp\left(-\int_0^a \mu(a')\,\mathrm{d}a'\right)$ denotes the probability that an individual infected a time units ago has not yet died. We will assume that infections are nonlethal, and this amounts to assuming a constant death rate: $\ell(a) = e^{-\mu a}$. We assume that the total host population remains constant, and the fraction of susceptible $S(t)$ obeys

$$\frac{dS}{dt} = \mu\,(1-S) - \lambda(t)\, S. \tag{10}$$

Approximation of epidemic sizes

For small enough patches, we consider the pathogen extinct in a patch when the fraction of infected hosts

$$H(t) = \int_0^{a_c} i(t,a)\,\mathrm{d}a,$$

reaches its first minimum value. We define the average duration of the epidemic $\bar{\delta}$ to be this duration by the time at which this occurs. Similarly, the average fraction of infected

$$\bar{\imath} = \frac{1}{\bar{\delta}} \int_0^{\bar{\delta}} H(t)\,\mathrm{d}t.$$

The patch-level net reproductive number is $R_* = \bar{\imath}\,\bar{\delta}\, m\, n$. The quantities $\bar{\imath}$ and $\bar{\delta}$ can be computed numerically either by simulation of the agent-based model or by numerical integration of Eqs. 8–10. Figure 7 shows estimates for R_* calculated both ways.

Sensitivity to birth and migration rates

To explore sensitivity to change in birth and migration rates, we take a metapopulation configuration ($N_P = 20$, and

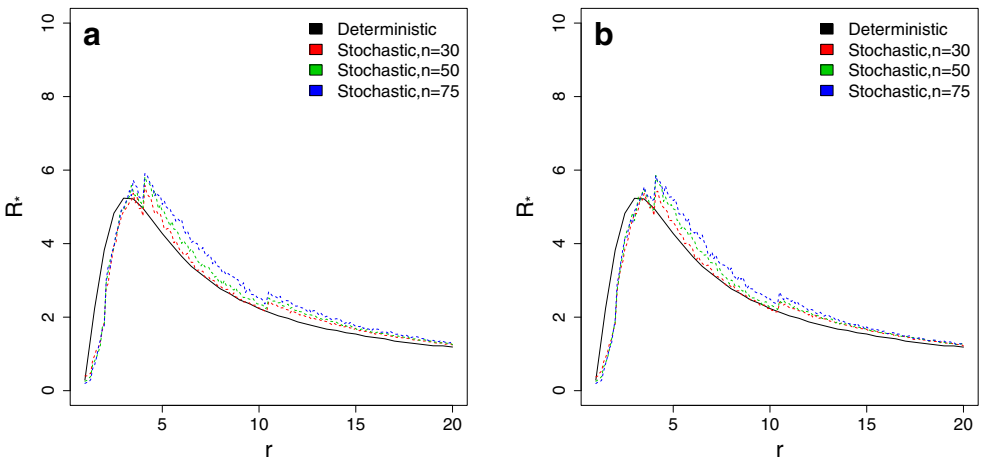

Fig. 7 Estimates of R_* for linear **a** and **b** saturating models, computed using both deterministic and stochastic frameworks. The curves are similar for both models, and each attains its maximum for $r \approx 3.5$

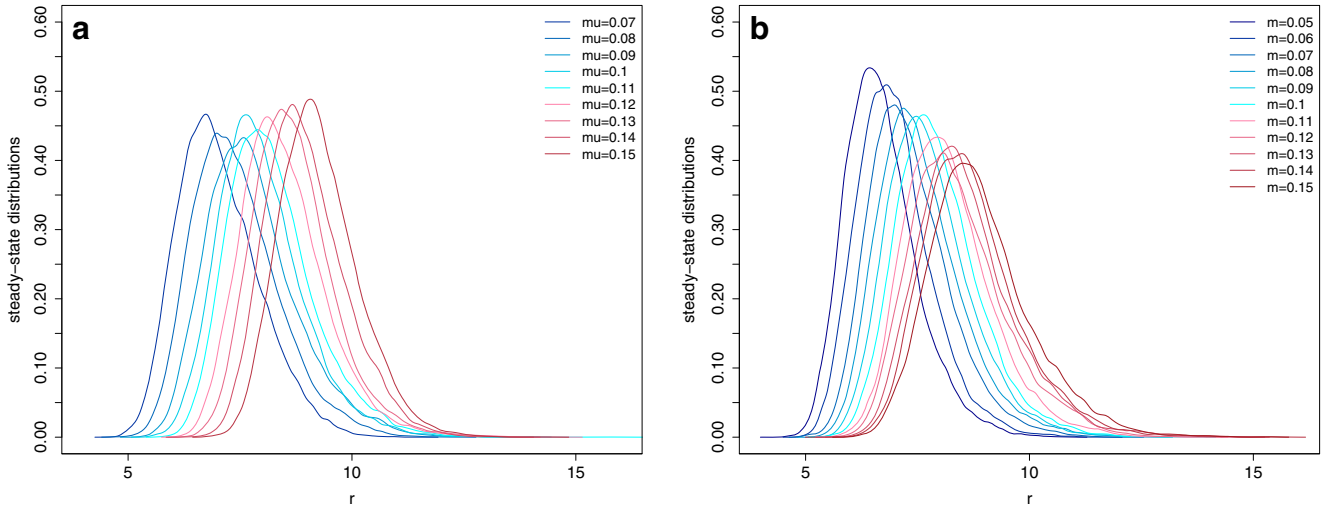

Fig. 8 Sensitivities to birth and migration. The graphs show the ESS r, with the metapopulation configuration $N_P = 20$ and $n = 100$, as **a** birth rate μ and **b** migration rate m vary. For each parameter value, 1,000 replicate simulations were performed in the same fashion as for figures in the main text

$n = 100$) and observe the change in the steady-state distributions of r. In Fig. 8, we see that increasing either migration or birth rates shifts the ESS r towards r^*. This is not surprising. Increasing either the birth rate or the migration rate sustains the epidemic locally for longer periods, allowing for within-patch competition to be more relevant.

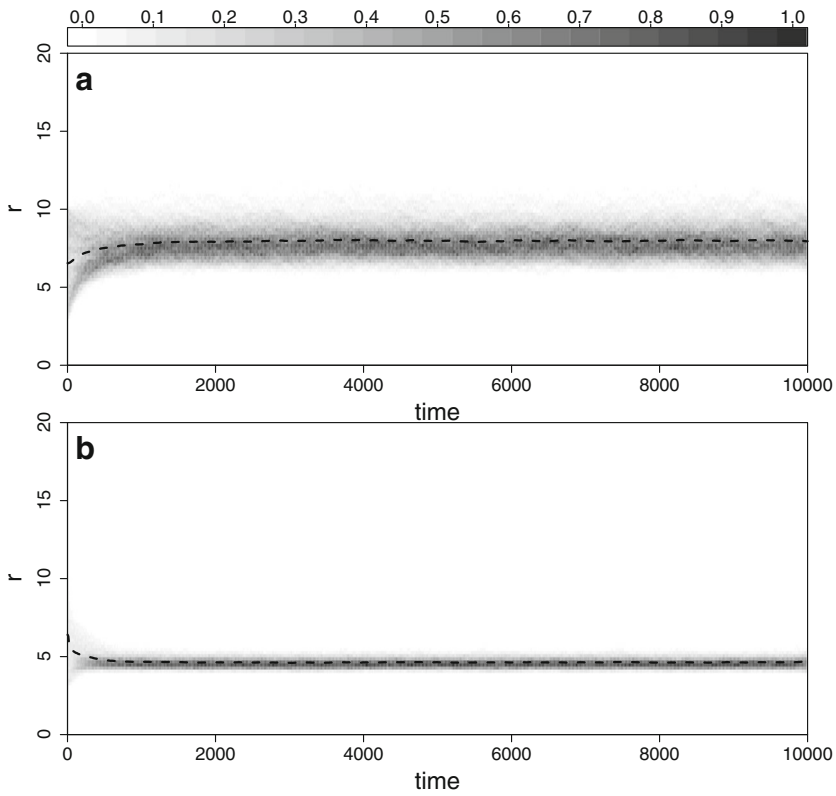

Fig. 9 Sample trajectories of pathogen evolution through time in two multi-patch configurations. **a** $N_P = 20$ and $n = 100$, and **b** $N_P = 300$ and $n = 20$. The *grayscale* indicates the distribution of $r(t)$ within the pathogen population; the *dashed line plots* the mean value of $r(t)$

Sample trajectories

We present sample trajectories for two chosen multi-patch configuration depicting the evolution of r over time. Compared to a single-patch dynamics that converges to ESS r that maximizes R_0 (as seen in Fig. 4), the trajectories converges to different ESS rs depending on patch configuration.

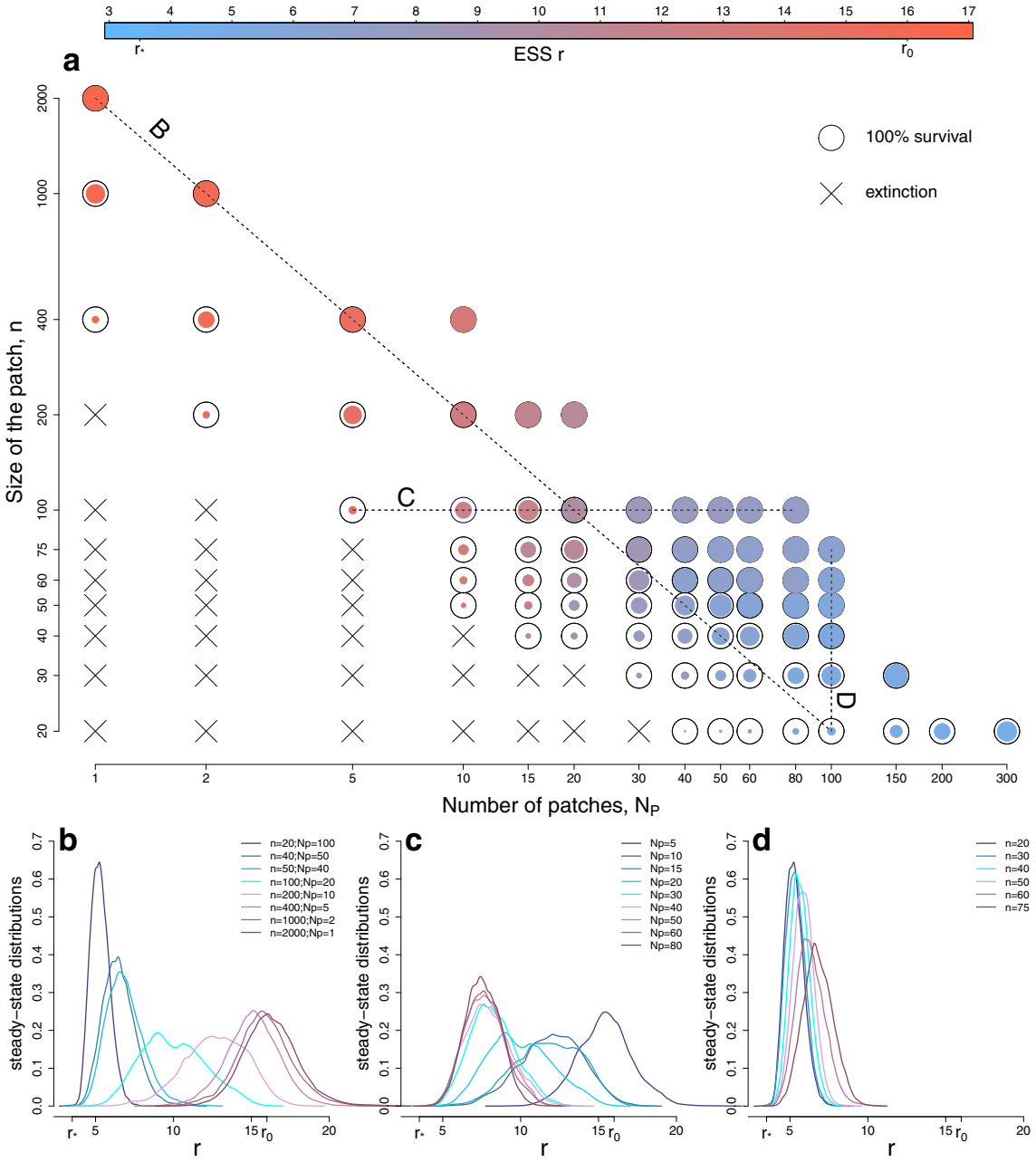

Fig. 10 Evolutionarily stable strategy (*ESS*) in populations without density dependence. This figure is comparable to Fig. 5 in the main text, except that here, the host mortality rate is held constant and equal to the host birth rate μ, (i.e., it is no longer density dependent). **a** ESS r (mean r in the stable strain distribution, indicated by *color*) and survival fraction (chance of avoiding extinction by time 2,000, indicated by *symbol size*), at various metapopulation configurations. Metapopulations are characterized by size of patch, n (*vertical axis*), and number of patches, N_P (*horizontal axis*). *Black crosses* indicate extinction in all of 1,000 replicate runs by time 2,000. The *bottom panels* show steady-state strain distributions along three different transects across metapopulation structure. **b** The size and the number of patches vary, and the expected total regional population size remains constant at 2,000. **c** The number of patches varies, and the expected size of each patch remains constant at 100. **d** The size of patches varies, and the number of patches remains constant. Metapopulations with many large patches were not explored due to computational infeasibility

Evolutionarily stable strategies in populations under pure birth–death process

Here, we relax the assumption of density-dependent mortality, by holding the host mortality constant and equal to the host birth rate, μ. In Fig. 10, comparable to Fig. 5 in the main text, we present the ESS as a function of host configuration. The notable difference is in transect C, in contrast to the observation in the main text; here, we see that changing the number of patches of size 100 decreases the ESS value of r.

References

Alizon S, van Baalen M (2005) Emergence of a convex trade-off between transmission and virulence. Am Nat 165(6):E155–E167. doi:10.1086/430053

Antia R, Levin BR, May RM (1994) Within-host population dynamics and the evolution and maintenance of microparasite virulence. Am Nat 144(3):457–472

Ball F, Neal P (2002) A general model for stochastic SIR epidemics with two levels of mixing. Math Biosci 180:73–102. doi:10.1016/S0025-5564(02)00125-6

Ball F, Mollison D, Scalia-Tomba G (1997) Epidemics with two levels of mixing. Ann Appl Probab 7:46–89. doi:10.1214/aoap/1034625252

van Ballegooijen WM, Boerlijst MC (2004) Emergent trade-offs and selection for outbreak frequency in spatial epidemics. Proc Natl Acad Sci USA 101(52):18,246–18,250. doi:10.1073/pnas.0405682101

Bjørnstad ON, Harvill ET (2005) Evolution and emergence of *Bordetella* in humans. Trends Microbiol 13(8):355–359. doi:10.1016/j.tim.2005.06.007

Bjørnstad ON, Finkenstädt BF, Grenfell BT (2002) Dynamics of measles epidemics: estimating scaling of transmission rates using a time series SIR model. Ecol Monogr 72(2):169–184. doi:10.1890/0012-9615(2002)072[0169:DOMEES]2.0.CO;2

Black F (1975) Infectious diseases in primitive societies. Science 187(4176):515–518. doi:10.1126/science.163483

Black FL, Hierholzer WJ, Pinheiro F, Evans AS, Woodall JP, Opton EM, Emmons JE, West BS, Edsall G, Downs WG, Wallace GD (1974) Evidence for persistence of infectious agents in isolated human populations. Am J Epidemiol 100(3):230–250

Boldin B, Diekmann O (2008) Superinfections can induce evolutionarily stable coexistence of pathogens. J Math Biol 56(5):635–672

Boots M, Sasaki A (1999) Small worlds and the evolution of virulence: infection occurs locally and at a distance. Proc R Soc Lond B 266(1432):1933–1933. doi:10.1098/rspb.1999.0869

Boots M, Hudson PJ, Sasaki A (2004) Large shifts in pathogen virulence relate to host population structure. Science 303(5659):842–844. doi:10.1126/science.1088542

Coombs D, Gilchrist M, Ball C (2007) Evaluating the importance of within- and between-host selection pressures on the evolution of chronic pathogens. Theor Popul Biol 72(4):576–591. doi:10.1016/j.tpb.2007.08.005

Cross PC, Lloyd-Smith JO, Johnson PLF, Getz WM (2005) Duelling timescales of host movement and disease recovery determine invasion of disease in structured populations. Ecol Lett 8(6):587–595. doi:10.1111/j.1461-0248.2005.00760.x

Cross PC, Johnson PLF, Lloyd-Smith JO, Getz WM (2007) Utility of R_0 as a predictor of disease invasion in structured populations. J R Soc Interface 4:315–324. doi:10.1098/rsif.2006.0185

Ewald PW (1993) The evolution of virulence. Sci Am 268:8

Ferrari M, Perkins S, Pomeroy L, Bjørnstad O (2011) Pathogens, social networks, and the paradox of transmission scaling. Interdisciplinary perspectives on infectious diseases 2011:267,049. doi:10.1155/2011/267049

Ganusov VV, Antia R (2003) Trade-offs and the evolution of virulence of microparasites: do details matter? Theor Popul Biol 64(2):211–220. doi:10.1016/S0040-5809(03)00063-7

Gilchrist MA, Coombs D (2006) Evolution of virulence: Interdependence, constraints, and selection using nested models. Theor Popul Biol 69(2):145–153. doi:10.1016/j.tpb.2005.07.002

Gilchrist MA, Sasaki A (2002) Modeling host-parasite coevolution: a nested approach based on mechanistic models. J Theor Biol 218(3):289–308. doi:10.1006/yjtbi.3076

Grenfell BT (2001) Dynamics and epidemiological impact of microparasites. In: l Smith G, Irving WL, McCauley JW, Rowlands DJ (eds) New challenges to health: the threat of virus infection. Cambridge University Press, Cambridge, pp 33–52

Higham DJ (2008) Modeling and simulating chemical reactions. SIAM Rev 50(2):347–368. doi:10.1137/060666457

Keeling MJ (2000) Evolutionary trade-offs at two time-scales: competition versus persistence. Proc R Soc Lond B 267:385–391. doi:10.1098/rspb.2000.1013

King AA, Shrestha S, Harvell ET, Bjørnstad ON (2009) Evolution of acute infections and the invasion-persistence trade-off. Am Nat 173:446–455. doi:10.1086/597217

Levin S, Pimentel D (1981) Selection of intermediate rates of increase in parasite-host systems. Am Nat 117(3):308–315

May RM, Anderson RM (1983) Parasite-host coevolution. In: Futuyma DJ, Slatkin M (eds) Coevolution, Sinauer. Mass, Sunderland

Mira A, Pushker R, Rodriguez-Valera F (2006) The Neolithic revolution of bacterial genomes. Trends Microbiol 14(5):200–206. doi:10.1016/j.tim.2006.03.001

Morozov A, Best A (2012) Predation on infected host promotes evolutionary branching of virulence and pathogens' biodiversity. J Theor Bio 307:29–36

Pilyugin SS, Antia R (2000) Modeling immune responses with handling time. Bull Math Biol 62:869–890. doi:10.1006/bulm.2000.0181

Rand DA, Keeling MJ, Wilson HB (1995) Invasion, stability and evolution to criticality in spatially extended, artificial host-pathogen ecologies. Proc R Soc Lond B 259:55–63. doi:10.1098/rspb.1995.0009

Svennungsen TO, Kisdi E (2009) Evolutionary branching of virulence in a single-infection model. J Theor Bio 257(3):408–418